M. Sakane and M. Ohnami**

High-Temperature Multiaxial Low-Cycle Fatigue

REFERENCE Sakane, M. and Ohnami, M., **High-temperature multiaxial low-cycle fatigue**, *Multiaxial Fatigue and Design*, ESIS 21 (Edited by A. Pineau, G. Cailletaud, and T. C. Lindley) 1996, Mechanical Engineering Publications, London, pp. 155–171.

ABSTRACT This paper describes a low-cycle fatigue criterion for tension–torsion and equibiaxial tension–compression low-cycle fatigue. The suitability of several multiaxial fatigue strain parameters is discussed by applying these parameters to the experimental data of heat resistant steels, conventional cast, directionally solidified and single-crystal superalloys. Anisotropic strain is proposed to correlate multiaxial low-cycle fatigue life of the directionally solidified and single-crystal superalloys. Also, nonproportional strain is proposed for the correlation of nonproportional low-cycle fatigue life under 13 strain paths.

1 Introduction

Development of an appropriate multiaxial low-cycle fatigue (LCF) strain parameter is needed for a proper design of components which receive multiaxial low-cycle fatigue damage at elevated temperatures. Von Mises equivalent strain has been used for the design basis but recent studies have demonstrated that von Mises strain is not always applicable to the multiaxial LCF data correlation.

The objective of this paper is to discuss the applicability of multiaxial strain parameters. Multiaxial strain parameters are applied to the experimental data and the suitability of the parameters is examined. Recent high-temperature materials have anisotropic deformation behaviour, for example, single-crystal (SC) and directionally solidified (DS) superalloy, so that multiaxial low-cycle fatigue parameter must take account of the anisotropy of materials.

2 Tension–Torsion High-Temperature Multiaxial Low-Cycle Fatigue

Figure 1 shows the correlation of the tension–torsion LCF data with von Mises strain for:

(a) Type 304 stainless steel (**1**);
(b) 1Cr–1Mo–(1/4)V steel (**2**);
(c) 63Sn–37Pb solder (**3**).

In these figures, solid lines are drawn based on the tension data and dotted lines indicate a factor of two scatter bands. Von Mises strain cannot correlate

*Ritsumeikan University, 1916 Noji-cho Kusatsu Shiga, 525, Japan.

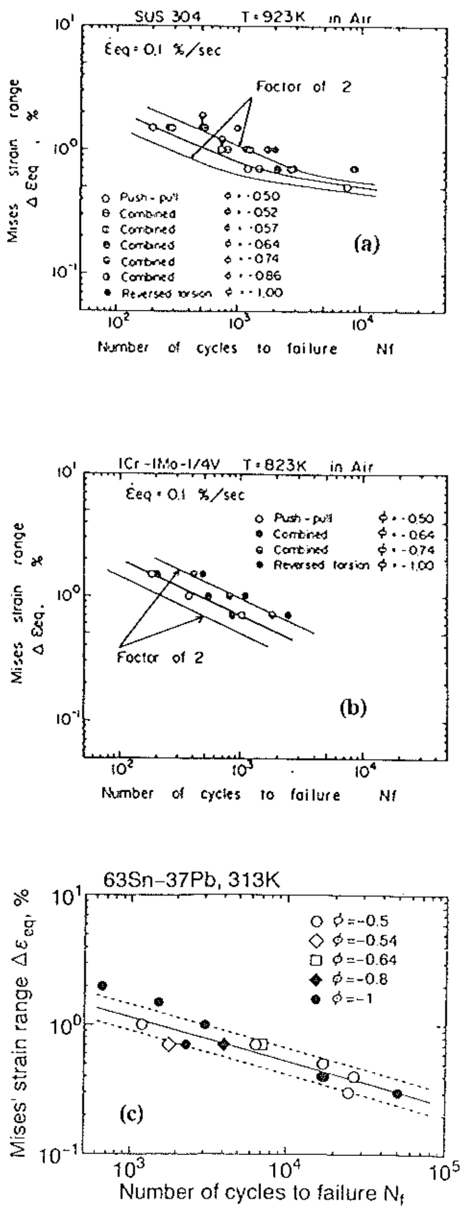

Fig 1 Correlation of tension–torsion multiaxial low-cycle fatigue life behaviour with von Mises strain for (a) Type 304 stainless steel; (b) 1Cr–1Mo–(1/4)V steel; (c) 63Sn–37Pb solder.

the tension–torsion multiaxial LCF lives within a factor of two scatter bands for Type 304 stainless steel. The torsion data are correlated conservatively and

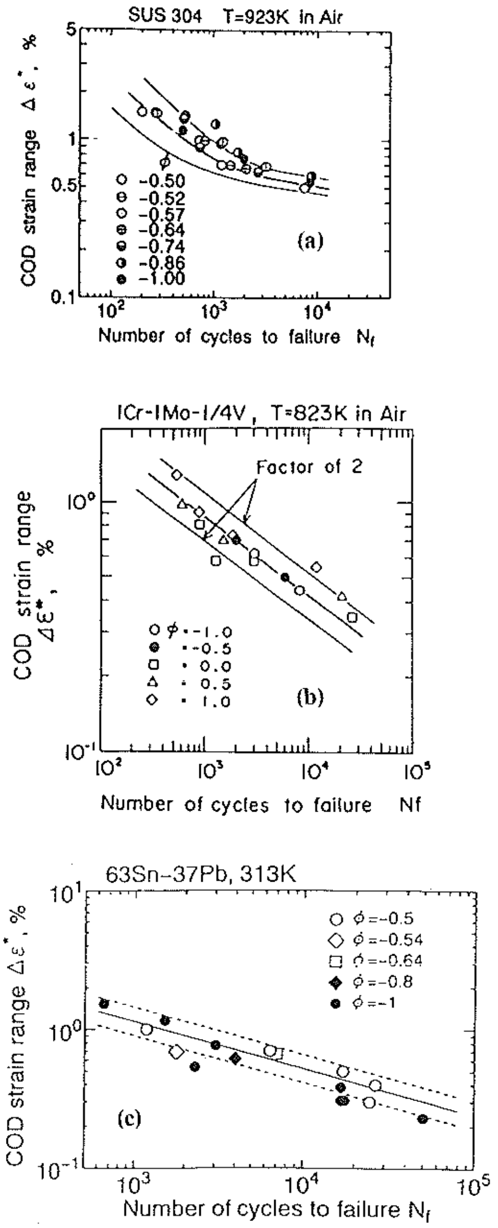

Fig 2 Correlation of tension–torsion multiaxial low-cycle fatigue life behaviour with COD strain for (a) Type 304 stainless steel; (b) 1Cr–1Mo–(1/4)V steel; (c) 63Sn–37Pb solder.

are out of a factor of two scatter bands. Von Mises strain also gives a similar correlation for 1Cr–1Mo–(1/4)V steel to Type 304 stainless steel, but the torsion

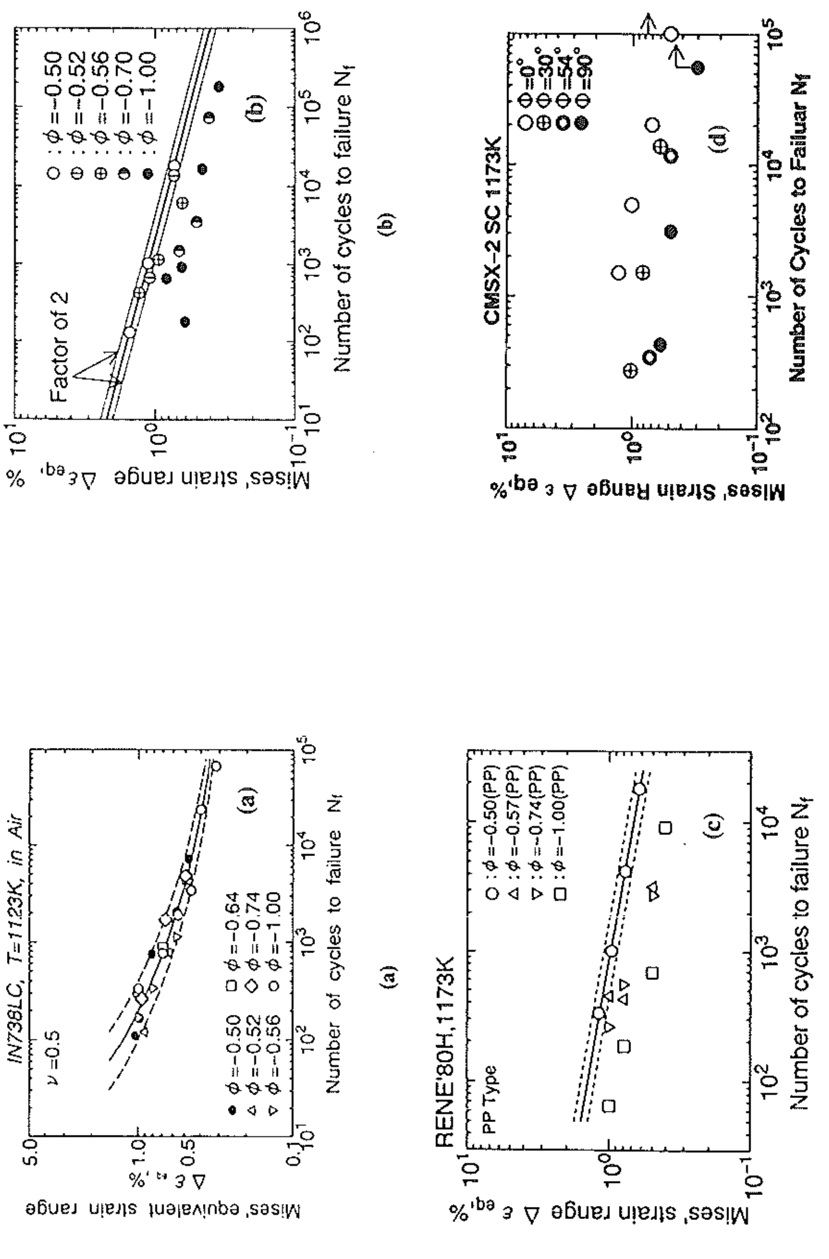

Fig 3 Correlation of tension–torsion multiaxial low-cycle fatigue lives with Mises strain for (a) Inconel 738LC superalloy; (b) Mar-M247LC directionally solidified superalloy; (c) Rene80 directionally solidified superalloy; (d) CMSX-2 single crystal superalloy.

data are just outside a factor of two scatter bands for 1Cr–1Mo–(1/4) steel. For 63Sn–37Pb solder, von Mises strain is a suitable parameter for the data correlation.

Figure 2 (4) also shows the same correlation as Fig. 1 but with the equivalent strain based on crack opening displacement (COD) strain. COD strain is expressed by the following equation

$$\Delta\varepsilon^* = \beta(2 - \phi)^{m'}\Delta\varepsilon_y$$
$$\beta = 1.83,\ m' = -0.66 \quad (1)$$

In the equation $\Delta\varepsilon_y$ is the maximum principal strain range and ϕ is the principal strain ratio defined as $\phi = \varepsilon_x/\varepsilon_y$; ε_y is the maximum principal strain and ε_x the minimum principal strain. The constants m′ and β do not depend on material. The COD strain shows a better correlation for Type 304 stainless steel in comparison with von Mises strain. The torsion data come into a factor of two scatter bands. The COD strain also shows a satisfactory data correlation for the other two materials.

Figure 3 shows the correlation of tension–torsion LCF fatigue lives for:

(a) Inconel 738LC conventional cast superalloy (5);
(b) Mar–M247LC directionally solidified superalloy (6);
(c) Rene80 directionally solidified superalloy (7);
(d) CMSX–2 single-crystal superalloy with von Mises strain (8).

Von Mises strain correlates Inconel 738LC conventional cast superalloy with a small scatter. For directional and single-crystal superalloys, on the other hand, von Mises strain is not suitable for the data correlation. Von Mises strain gives a large scatter of the data. The torsion LCF data locate unconservatively in comparison with the tension data. The torsion data for SC superalloy are more unconservatively correlated than those for DS superalloy. The inappropriate data correlation for DS and SC superalloys is resulted from the anisotropy of deformation behaviour of such materials.

Figure 4 shows the stress–total strain relation on von Mises equivalent basis for CMSX–2 single-crystal superalloy. Von Mises stress increases with decreasing principal strain ratio. This stress increase is caused by the anisotropy of Young's modulus. Understanding of anisotropy of Young's modulus is essential for the life prediction of DS and SC superalloys.

Figure 5 shows the variation of Young's modulus with θ and ϕ for pure nickel. The heavy line in the figure indicates the specimen axis. The angles θ and ϕ are the deviation angle from [001] axis and the rotation angle about the specimen axis, respectively. The Young's modulus increases with increasing θ and the increased ratio is larger for larger ϕ up to $\theta = 45$ degrees. The anisotropy of Young's modulus should be taken into account in the multiaxial strain parameter. This paper proposes the following strain parameter for correlating multiaxial LCF data for DS and SC superalloys (8).

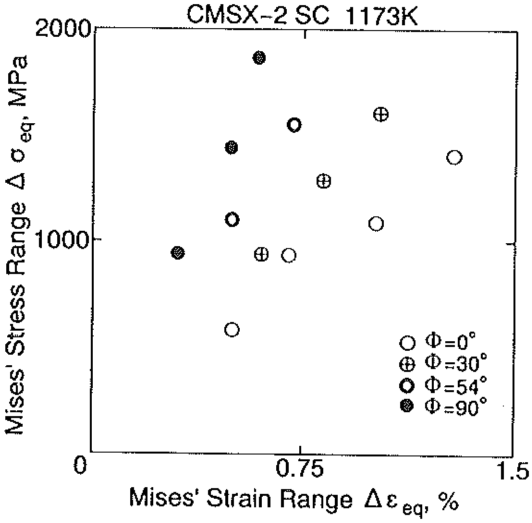

Fig 4 Mises equivalent stress – Mises' total strain relation for CMSX-2 single crystal supperalloy.

$$\Delta\varepsilon_{an} = \frac{E(\alpha, \beta)}{E_0} \Delta\varepsilon_1 \qquad (2)$$

In the equation $\Delta\varepsilon_{an}$ is the anisotropic strain range proposed here and $\Delta\varepsilon_1$ is the maximum principal strain range. E_0 is Young's modulus in [001] direction and $E(\alpha, \beta)$ is that in the maximum principal direction. The angle α is taken as

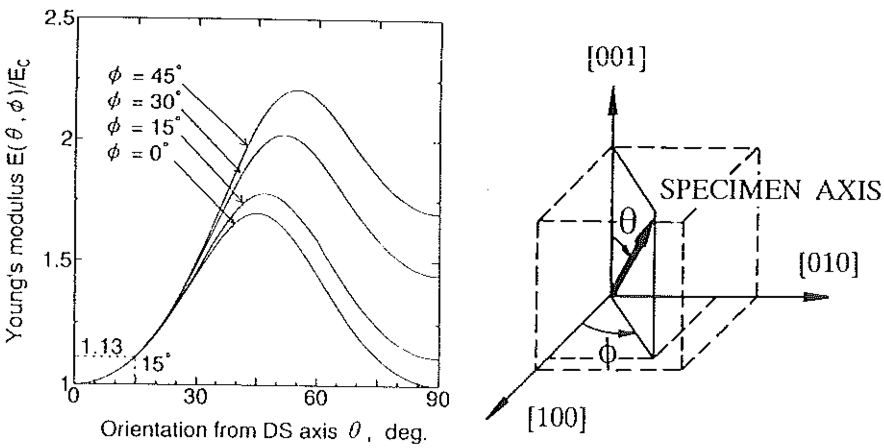

Fig 5 Variation of Young's modulus with θ and ϕ together with the definition of two angles.

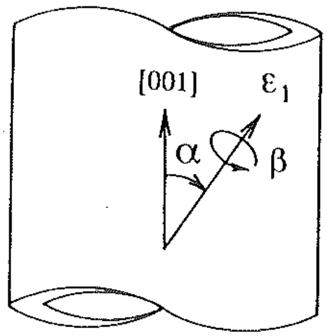

Fig 6 Definition of angles α and β in anisotropic strain range.

the angle between the specimen axis and principal strain direction as shown in Fig. 6. The angle β is randomly distributed so that the mean value of 25.0 degrees was employed in this paper.

Figure 7 correlates the LCF lives with the anisotropic strain expressed by equation (2). For the two DS superalloys, the correlation of the data is satisfactory and almost all of the data are located within a factor of two scatter bands. For SC superalloy, the anisotropic strain is also suitable but the torsion data are slightly out by a factor of two scatter bands. The degree of anisotropy is stronger in SC superalloy in comparison with DS superalloy.

3 Equibiaxial Tension–Compression Multiaxial Low-Cycle Fatigue Using Cruciform Specimens

Tension–torsion LCF studies have been made for developing a suitable multiaxial strain parameter but tension–torsion tests only enable experiments in limited multiaxial stress/strain states. Experimental verification in more widely ranged multiaxial stress states is required. The authors have developed a high-temperature multiaxial LCF machine for cruciform specimens, the geometry of which is shown in Fig. 8 (9).

Figure 9 (9) shows the LCF life behaviour of Type 304 cruciform specimens with the principal strain range in the y-direction. In the figure, the $\phi = -1$ test corresponds to the torsion test and the $\phi = 1$ test is the equibiaxial tension–compression test. LCF life decreases with increasing principal strain ratio in $\Delta\varepsilon_y$ constant tests.

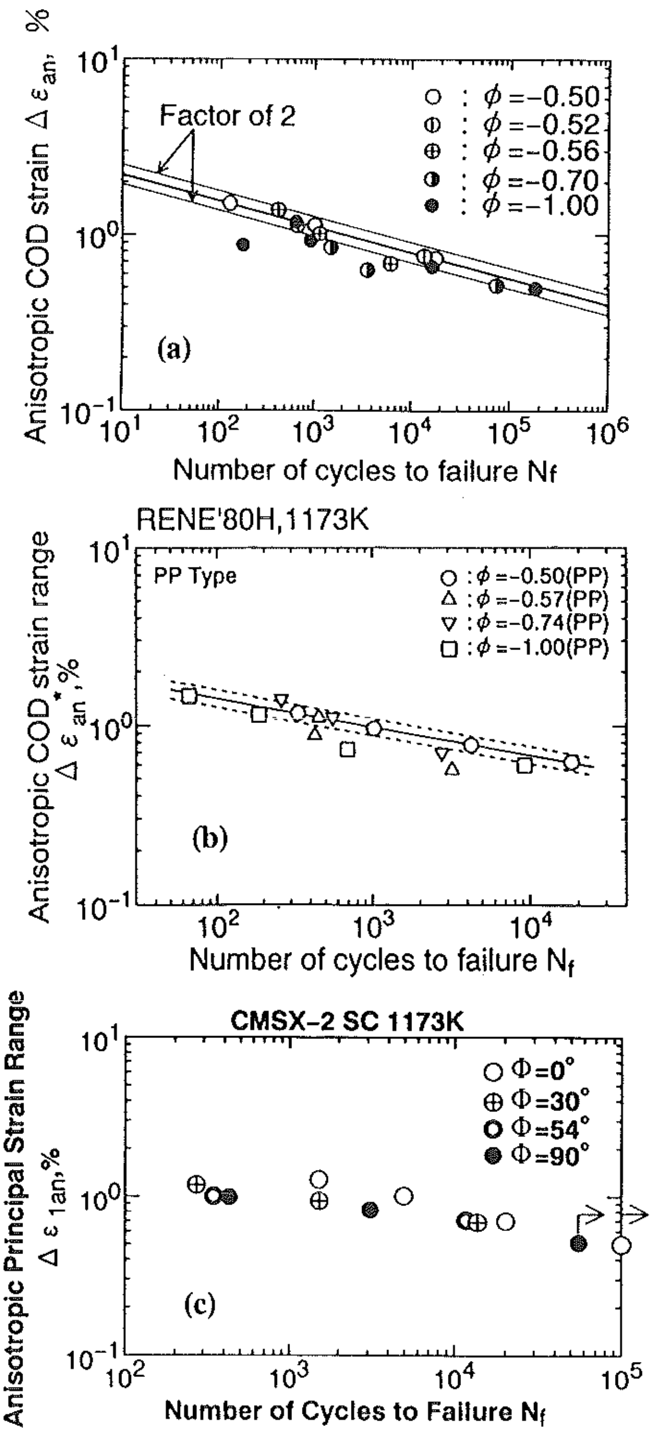

Fig 7 Correlation of tension-torsion LCF data for (a) Mar-M247LC DS superalloy; (b) Rene 80 DS superalloy; (c) CMSX-2 SC superalloy with anisotropic strain.

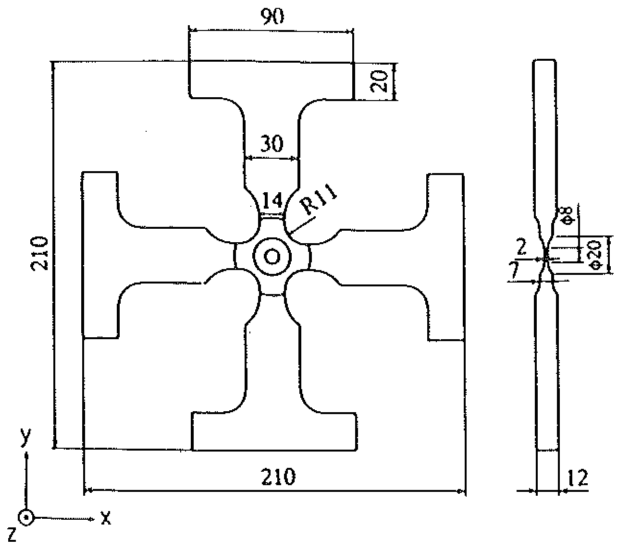

Fig 8 Shape and dimensions of cruciform specimen.

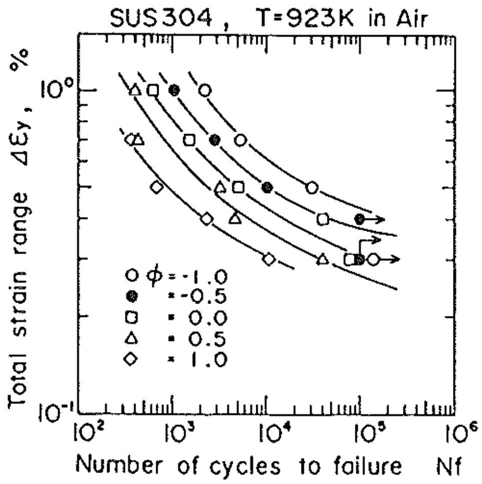

Fig 9 Low-cycle fatigue life behaviour of Type 304 cruciform specimens in $\Delta\varepsilon_y$ constant tests.

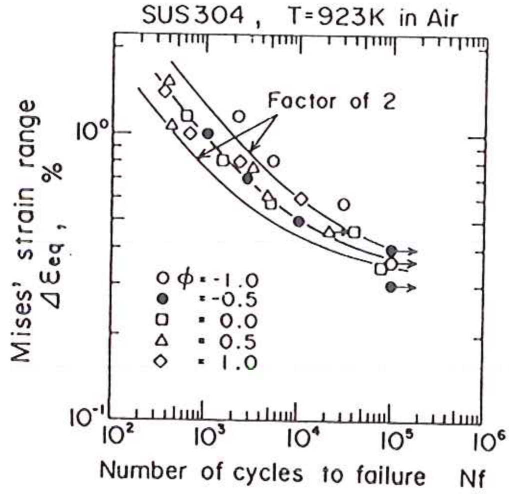

Fig 10 Correlation of multiaxial LCF lives with von Mises strain

The data correlation with von Mises strain is shown in Fig. 10 (9). Von Mises strain cannot correlate the multiaxial LCF lives in the range of principal strain ratio between -1 and 1 within a small scatter. The $\phi = -1$ data are located unconservatively. Figure 11 (9) also shows the data correlation with COD

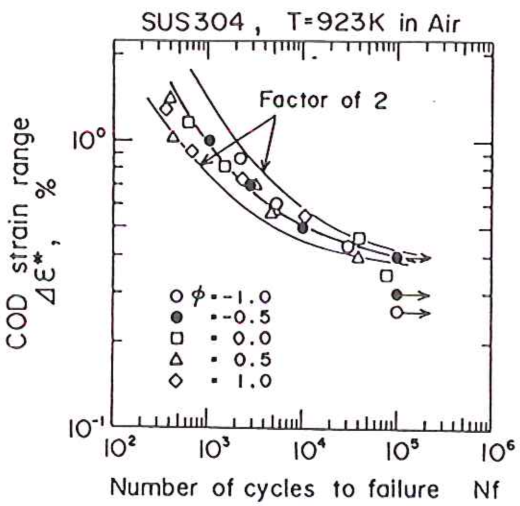

Fig 11 Correlation of multiaxial LCF lives with COD strain.

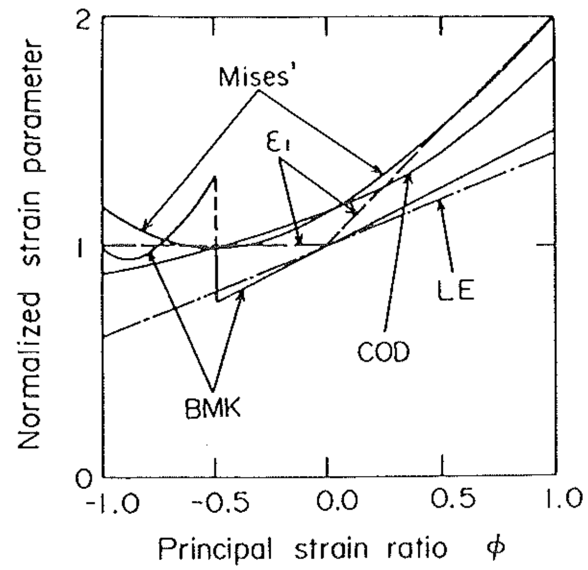

Fig 12 Comparison of multiaxial strain parameters.

strain range. Most of all the data are within a factor of two scatter bands.

Figure 12 (9) compares several multiaxial strain parameters. The ordinate is normalized by the principal strain. The test results of cruciform specimens showed that the LCF life decreases with increasing ϕ, so that the appropriate parameter for correlating the multiaxial LCF data should increase with increasing ϕ in Fig. 12. The parameter which meets this condition is only COD strain. The Γ^*-parameter proposed by Lohr and Ellison (10) also meets this condition but the Γ^*-parameter does not agree with the value of maximum principal strain in uniaxial tests. Von Mises strain is appropriate in the principal strain ratio of $-0.5 < \phi \leqslant 1$ but disagrees with the experimental data in the principal strain ratio range of $-1 \leqslant \phi \leqslant -0.5$. In this range, von Mises strain decreases with increasing ϕ so that the data correlation with von Mises strain is not satisfactory.

4 Nonproportional Low-Cycle Fatigue

Nonproportional loading sometimes occurs in practical components under the combined loading of mechanical and thermal stresses. ASME Code Case (11) has been used as a design criterion for nonproportional fatigue, but recent studies have shown that the Code Case estimates unconservative lives for the nonproportional fatigue. In order to examine the effect of nonproportional loading on fatigue life behaviour, fatigue tests under 13 nonproportional strain

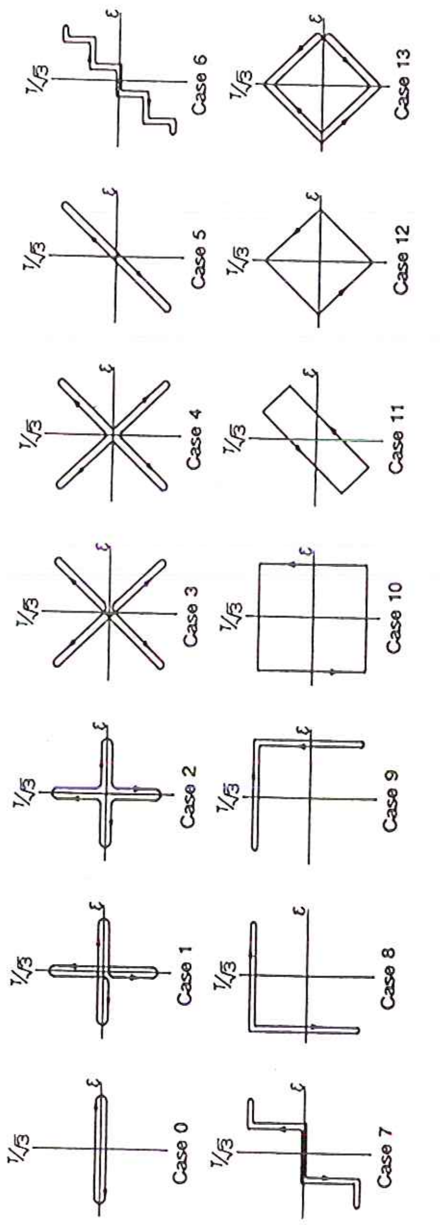

Fig 13 Strain paths employed in nonproportional LCF tests.

paths were carried out for Type 304 stainless steel hollow cylinder specimens (O.D. 11 mm, I.D. 9 mm, G.L. 4.2 mm) at room temperature (**12**). The 13 strain paths are shown in Fig. 13 (**12**). The 13 strain paths were programmed to help study several effects of nonproportional loading shown in Table 1 (**12**).

Table 1 Nonproportional factors examined in 13 strain paths

Aspect	*Strain path number*
Effect of two principal strain directions	0↔1, 2 5↔3, 4
Effect of out-of-phase loadings (0°, 45°, 90°)	5↔11↔12
Full reversed loading or zero-to-maximum loading	1↔2 3↔4
Mean strain effect	1↔8, 9 8↔9 8↔9↔10
Step length effect	5↔6↔7↔8, 9
Rotating or turn around loading	12↔13

Tables 2 and 3 (**12**) list fatigue life in cases 0 and 13 nonproportional tests. Nonproportional tests were carried out at two strain ranges of 0.5% and 0.8% to confirm the characteristics of fatigue life behaviour in elastic and plastic dominant regions. In all the 13 strain paths, the normal strain had the same amplitude as the shear strain on von Mises basis. A complete loading along the strain paths shown in Fig. 13 was counted as one cycle for all the cases except case 3, 4 and 13. In cases 3, 4 and 13 a complete loading was counted as two cycles.

Table 2 Fatigue lives in Case 0 tests

Strain range $\Delta\varepsilon$ (%)		0.5	0.65	0.8	1.0	1.2	1.5
Path number	Case 0	49 000	23 400	7100	1500	690	540

Table 3 Summary of fatigue lives under 13 nonproportional loadings

Path number (Case)		1	2	3	4	5	6	7	8	9	10	11	12	13
Strain range $\Delta\varepsilon$ (%)	0.5	9500	20 000	2400	3400	17 500	9700	18 000	2050	2950	2600	14 400	4750	3200
	0.8	1260	2100	820	900	3200	2700	1700	470	660	320	1930	710	1000

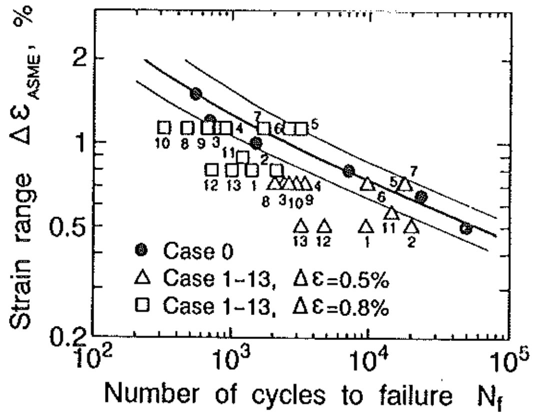

Fig 14 Correlation of nonproportional LCF lives with ASME strain.

Figure 14 (**12**) correlates the nonproportional LCF lives with the equivalent strain recommended by ASME Code Case (**11**). In the figure, a factor of two scatter bands is shown by the lines based on the tension data, i.e., case 0 data. The equivalent strain in the Code Case is expressed as

$$\Delta\varepsilon_{ASME} = \mathrm{Max}[\{(\varepsilon_A - \varepsilon_B)^2 + (\gamma_A - \gamma_B)^2/3\}^{1/2}] \tag{3}$$

Fatigue lives for cases 5-7 and for case 11 locate within a factor of two scatter bands. The fatigue data in all the other strain paths are correlated unconservatively. Especially, fatigue lives of cases 3, 4, 12 and 13 are 8–30 percent of those in case 0. Thus, the life prediction based on the ASME Code Case for nonproportional loading becomes unconservative for most of the strain paths.

This paper proposes a new nonproportional parameter, $\Delta\varepsilon_{NP}$, expressed by the following equation (**12**)

$$\Delta\varepsilon_{NP} = (1 + \alpha \cdot f_{NP})\Delta\varepsilon_I \tag{4}$$

where α is a material constant related to the additional hardening under nonproportional loading. f_{NP} is the nonproportional factor which expresses the severity of nonproportional loading and is described only by the strain history. $\Delta\varepsilon_I$ is the maximum principal strain range under nonproportional loading. For Type 304 stainless steel, α is equal to 0.9.

The nonproportional factor is defined as

$$f_{NP} = \frac{k}{T \cdot \varepsilon_{Imax}} \int_0^T (|\sin(\xi(t))| \cdot \varepsilon_I(t))\, dt \tag{5}$$

$$k = 1.57$$

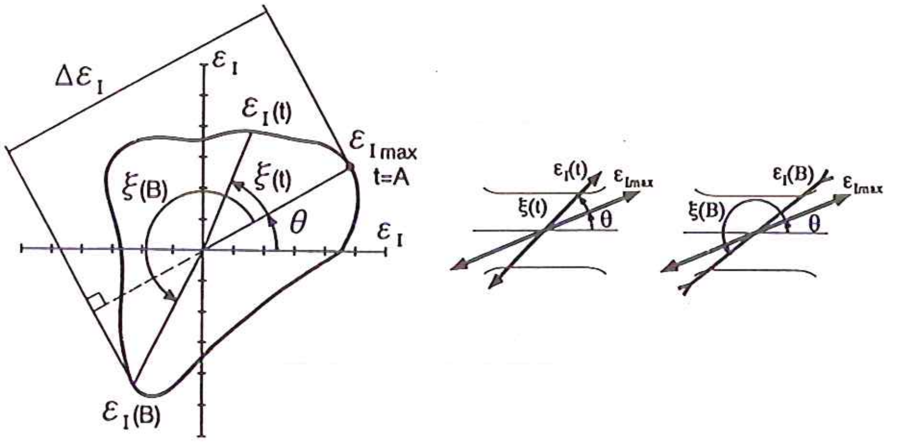

Fig 15 **Definition of $\varepsilon_I(t)$, ε_{Imax} and $\xi(t)$.**

In the equation, $\varepsilon_I(t)$, ε_{Imax} and $\xi(t)$ are the parameters defined in equations (6) and (7) (see Fig. 15). T is the time for a cycle. f_{NP} is a nondimensional value normalized by T and ε_{Imax}. k is a constant to make f_{NP} unity under 90 degrees out of phase loading: its value is 1.57

$$\Delta\varepsilon_I = \text{Max}[\varepsilon_{Imax} - \cos(\xi(t)) \cdot \varepsilon_I(t)] \tag{6}$$

$$\varepsilon_I(t) = \text{Max}[\,|\varepsilon_1(t)|, |\varepsilon_3(t)|\,] \tag{7}$$

Figure 16 (**12**) correlates the nonproportional fatigue lives with the nonproportional strain parameter shown in equation (4). Almost all the nonproportional data are within a factor of two scatter bands in the correlation with the nonproportional strain. Therefore, the nonproportional strain proposed by equation (4) is able to predict nonproportional LCF lives with various strain histories. This equation has only one material constant which is determined by the stress range ratios under 90 degrees out-of-phase and proportional loadings.

It should be noted that the nonproportional strain in equation (4) is based on the maximum principal strain. The nonproportional strain correlates well the nonproportional LCF life behaviour but it will not correlate proportional LCF life at various principal strain ratios (**11**). For correlating nonproportional LCF life including proportional fatigue life behaviour, nonproportional strain based on COD strain has been proposed in a somewhat different form from equation (4) (**12**).

5 Conclusions

The suitability of a multiaxial strain parameter is material dependent. Von Mises equivalent strain is not suitable for the data correlation of Type 304

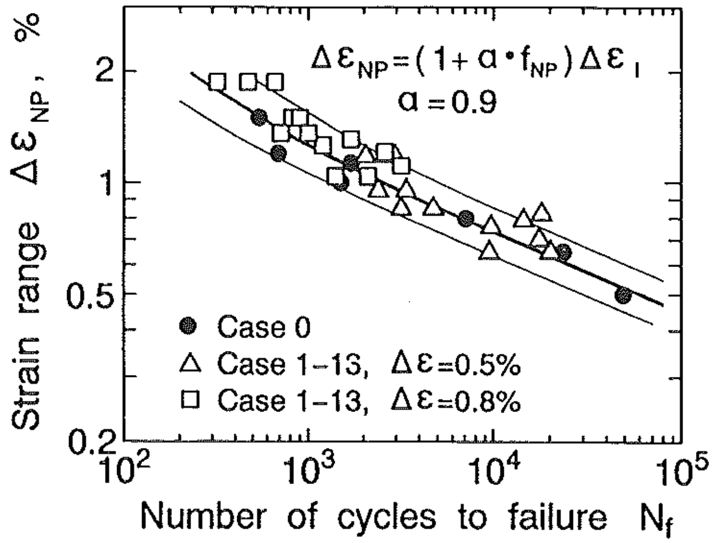

Fig 16 Correlation of nonproportional LCF life behaviour with nonproportional strain.

stainless steel and 1Cr–1Mo–(1/4)V steel, but is suitable for that of 63Sn–37Pb solder. For all of these materials, the equivalent strain based on COD is suitable.

Multiaxial LCF life behaviour using cruciform specimens is described. The strain biaxiality ratio has a significant influence on LCF life. The multiaxial strain parameter which correlates multiaxial LCF life including equibiaxial tension–compression life is COD strain and Γ*-parameter.

Von Mises strain is suitable for the data correlation of Inconel 738LC superalloy but is not suitable for DS and SC superalloys. Anisotropic strain parameter is proposed to correlate DS and SC superalloys, which takes account of the anisotropy of Young's modulus. Anisotropic strain correlates the LCF lives of DS and SC superalloys with a small scatter.

Nonproportional strain parameter is proposed. The proposed strain parameter is a function of only strain path except for one material constant. The nonproportional strain correlates the nonproportional fatigue life behaviour under 13 strain paths within a small scatter band.

References

(1) SAKANE, M., OHNAMI, M. and SAWADA, M. (1987) Fracture mode and low cycle fatigue life in biaxial stress state at elevated temperature, *Trans. ASME, JEMT*, **109**, pp. 236–243.

(2) SAKANE, M., OHNAMI, M. and SAWADA, M. (1991) Biaxial low cycle fatigue of unaged and aged 1Cr–1Mo–1/4V steels at elevated temperature, *Trans. ASME, JEMT*, **113**, pp. 244–253.

(3) YAMAMOTO, T., SAKANE, M., OHNAMI, M. and YAMADA, T. (1993) Multiaxial low cycle fatigue of 63Sn–37Pb solder for electric devices at elevated temperature, *Proc. 31st Symp. Strength Mater. at High Temp.*, JSMS, pp. 94–98.

(4) OHNAMI, M. and SAKANE, M. (1992) Design criteria for multiaxial creep-fatigue, *Proc. 5th Inter. Conf. Creep*, ASM, pp. 13–22.
(5) ISOBE, N. (1993) Tension–torsion multiaxial creep-fatigue of Inconel 738LC superalloy, Master Thesis Ritsumeikan Univ.
(6) SHIMOMIZUKI, K., SHIRAFUJI, N., SAKANE, M. and OHNAMI, M. (1991) High temperature multiaxial low cycle fatigue of Mar–M247 directionally solidified Ni-base superalloy, *Proc. 29th Symp. Strength Mater. at High Temp.*, JSMS, pp. 21–25.
(7) HIROSE, T., SAKANE, M., OHNAMI, M., FUJIYAMA, K. and OKABE, N. (1993) Multiaxial creep-fatigue for Rene80H DS superalloy at elevated temperature, *Proc. 71th Ann. Meeting of JSME*, No. 930–63B, pp. 485–487.
(8) SHIRAFUJI, N., SHIMOMIZUKI, K., SAKANE, M. and OHNAMI, M., Tension–torsion multiaxial low cycle fatigue of Mar-M247 directionally solidified superalloy at elevated temperature, *Trans. ASME JEMT* (submitted).
(9) ITOH, T., SAKANE, M. and OHNAMI, M. (1994) High temperature multiaxial low cycle fatigue of cruciform specimen, *Trans. ASME. JEMT*, **116**, pp. 90–98.
(10) LOHR, R. D. and ELLISON, E. G. (1980) A simple theory of low cycle multiaxial fatigue, *Fatigue Eng. Mater. Tech.*, **3**, pp. 1–17.
(11) Cases is ASME Boiler and Pressure Vessel Code, Case N–47, Class 1, Section 3, Division 1, ASME, 1978.
(12) ITOH, T., SAKANE, M., OHNAMI, M. and SOCIE, Nonproportional low cycle fatigue criterion for Type 304 stainless steel, *Trans. ASME, JEMT*, **117**, 285–292.